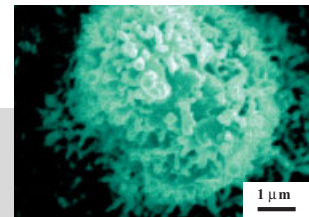


Super-Hydrophobic Surfaces: From Natural to Artificial**

By Lin Feng, Shuhong Li, Yingshun Li, Huanjun Li, Lingjuan Zhang, Jin Zhai, Yanlin Song, Biqian Liu, Lei Jiang,* and Daoben Zhu

Super-hydrophobic surfaces, with a water contact angle (CA) greater than 150°, have attracted much interest for both fundamental research and practical applications. Recent studies on lotus and rice leaves reveal that a super-hydrophobic surface with both a large CA and small sliding angle (α) needs the cooperation of micro- and nanostructures, and the arrangement of the microstructures on this surface can influence the way a water droplet tends to move. These results from the natural world provide a guide for constructing artificial super-hydrophobic surfaces and designing surfaces with controllable wettability. Accordingly, super-hydrophobic surfaces of polymer nanofibers and differently patterned aligned carbon nanotube (ACNT) films have been fabricated.



1. Introduction

The wettability of solid surfaces is a very important property, and is governed by both the chemical composition and the geometrical microstructure of the surface.^[1] The generation by UV illumination of a super-hydrophilic TiO₂ surface with a contact angle (CA) for water of 0° has attracted significant attention.^[2] This material has already been successfully applied as a transparent super-hydrophilic coating with anti-fogging and self-cleaning properties.^[3] Currently, super-hydrophobic surfaces with water CA higher than 150° are arousing much interest because they will bring great convenience in daily life as well as in many industrial processes.^[4] Various phenomena, such as snow sticking, contamination or oxidation, and current conduction, are expected to be inhibited on such a surface.^[5]

Conventionally, super-hydrophobic surfaces have been produced mainly in two ways. One is to create a rough structure

on a hydrophobic surface (CA > 90°), and the other is to modify a rough surface by materials with low surface free energy. Up to now, many methods have been developed to produce rough surfaces, including solidification of melted alkylketene dimer (AKD, a kind of wax),^[6] plasma polymerization/etching of polypropylene (PP) in the presence of polytetrafluoroethylene (PTFE),^[7] microwave plasma-enhanced chemical vapor deposition (MWPE-CVD) of trimethylmethoxysilane (TMMOS),^[8] anodic oxidation of aluminum,^[9] immersion of porous alumina gel films in boiling water,^[10] mixing of a sublimation material with silica or boehmite,^[5] phase separation,^[11] and molding.^[12] To obtain super-hydrophobic surfaces, coating with low-surface-energy materials such as fluoroalkylsilane (FAS) is often necessary.^[5,9–12] While the water CA has commonly been used as a criterion for the evaluation of hydrophobicity of a solid surface, this alone is insufficient to assess the sliding properties of water droplets on the surface.^[13] A fully super-hydrophobic surface should exhibit both high CA and low sliding angle (α), where α can also be expressed as the difference between advancing and receding contact angle (hysteresis).

2. The Effect of a Multiscale Plant Surface on Anti-Adhesion of Water

The self-cleaning effect of some plant leaves is of great interest for practical applications. The observation of hydropho-

[*] Prof. L. Jiang, Dr. L. Feng, Dr. S. Li, Y. Li, Dr. H. Li, L. Zhang, Dr. J. Zhai, Prof. Y. Song, B. Liu, Prof. D. Zhu
Center of Molecular Sciences, Institute of Chemistry
Chinese Academy of Sciences
Beijing 100080 (PR China)
E-mail: jianglei@infoc3.icas.ac.cn

[**] The authors thank the State Key Project for Fundamental Research (G1999064504) and the Special Research Foundation of the National Natural Science Foundation of China (20125102) for continuing financial support.

bicity related to the topology of the surface of a plant leaf was previously reported by Barthlott and Neinhuis.^[14] It was believed that this unique property is based on surface roughness caused by the micrometer-scale papillae and the epicuticular wax.^[15] However, the fundamental mechanism remains unclear. Recently, we reported a novel finding of micro- and nanoscale hierarchical structures on the surface of a lotus leaf, i.e., branch-like nanostructures on top of the micropapillae.^[16] These structures can induce super-hydrophobic surfaces with large CA and small α . Figure 1a shows a typical large-scale

scribe the relationship between CA on a rough surface (θ_f) and that on a smooth surface of the same solid (θ):

$$\cos \theta_f = f_s (L/l)^{D-2} \cos \theta - f_v \quad (1)$$

Here, $(L/l)^{D-2}$ is the surface roughness factor, where L and l are, respectively, the upper and lower limit scales of the fractal behavior of the surface, and D is the fractal dimension. In the case of the lotus leaf, L and l correspond to the size of the diameters of the papillae and branch-like nanostructures, respectively. In the triadic Koch curve model, the value of D in three-dimensional space was found to be about 2.2618, and the value of L/l equal to 3^n . The value of n is determined by the object acting on the fractal structures. The surface roughness factor became larger with increasing n value. Accordingly, if the upper limit scale L is certain, the larger the value of n , the smaller that of l . In Equation 1, f_s and f_v are the fractions of the surface under the water droplet occupied by solid material and air, respectively ($f_s + f_v = 1$). Here f_s and f_v were evaluated from the SEM image (Fig. 1a) as 0.2056 and 0.7944, respectively, and the value of θ was $104.6^\circ \pm 0.5^\circ$ measured from the primary component of epicuticular waxes.^[19] Therefore, the value of θ_f can be calculated from Equation 1 as 147.8° , 149.7° , 152.4° , 156.5° , and 163.4° for $n=0, 1, 2, 3,$ and 4 , respectively. Using these results, the contact angle (θ) was plotted as a function of diameter as in Figure 1d. The point corresponding to the situation on the surface of a lotus leaf can be found on the curve. CA was about 160° , from which the diameter was about 128 nm, in the scale of nanostructure. This model can be applied to all types of hydrophobic surfaces.

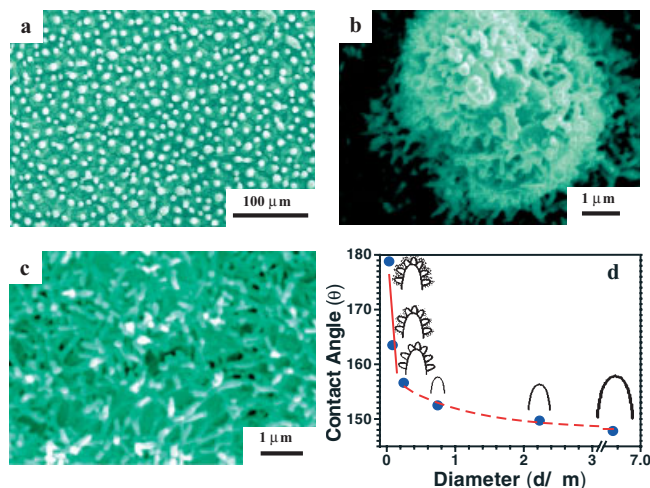


Fig. 1. a) Large-area SEM image of the surface of a lotus leaf (*Nelumbo nucifera*). Every epidermal cell forms a papilla and has a dense layer of epicuticular waxes superimposed on it. b) Enlarged view of a single papilla from (a). Reproduced from [16] with permission from the Chinese Physical Society. c) SEM image of the lower surface of the lotus leaf. d) The fitted curve based on calculated data (contact angle, in degrees, against the mean outer diameter of protruding structures, in micrometers).

scanning electron microscopy (SEM) image of the surface of a lotus leaf. Many papillae were found on this surface in a random distribution with diameters ranging from 5 to 9 μm . CA and α on the surface of this lotus leaf were about $161.0^\circ \pm 2.7^\circ$ and 2° , respectively. Figure 1b shows a high-resolution SEM (HRSEM) image of a single papilla, where hierarchical structures in the form of branch-like nanostructures with average diameters of 124.3 ± 3.2 nm on every papilla are clearly observed. Nanostructures were also found on the lower surface of the lotus leaf (Fig. 1c), which would effectively prevent the attachment of water droplets here also, should the underside of the leaf get wet. These nanostructures on the surface of the lotus leaf, especially on the top of the micropapillae, may be very useful for super-hydrophobicity.

A model of such a surface with super-hydrophobicity and multiscale character can be inferred as described by Adamson and Gast.^[17] The surface roughness was considered on the top of the papillae. Since the hierarchical structures on the surface of the lotus leaf are very similar to the description of the triadic Koch curve in fractal geometry,^[18] the fractal formula was used to calculate the roughness factor. By changing the roughness factor, a mathematic model was evolved as follows to de-

3. High Contact Angle Induced by Nanostructures

Nanostructures on a solid surface are very important for super-hydrophobicity, which can induce a high CA. Recently, we reported the preparation of densely packed aligned carbon nanotube (ACNT) films with pure nanostructures.^[20] Figures 2a and 2b show SEM images of the top and cross-sectional views of the as-grown densely packed ACNTs, respectively. These nanotubes are aligned almost normal to the substrate surface with a fairly uniform external diameter of about 60 nm. The CA on these nanostructured ACNT films was $158.5^\circ \pm 1.5^\circ$. Furthermore, the as-grown ACNT films exhibited super-“amphiphobicity” after fluoroalkylsilane coating, that is, CAs for both water and oil were larger than 160° . This phenomenon was believed to be due to the nanostructures and the presence of fluoroalkylsilane groups. Based on this study, we are currently developing a novel template-based extrusion method to synthesize a super-hydrophobic surface of polyacrylonitrile (PAN) nanofibers.^[21] Figure 2c shows a cross-sectional SEM image of as-synthesized PAN nanofibers. Aligned PAN nanofibers with end tips were obtained, the average diameter of the nanofiber tips and interfiber distance being about 104.6 nm and 513.8 nm, respectively.

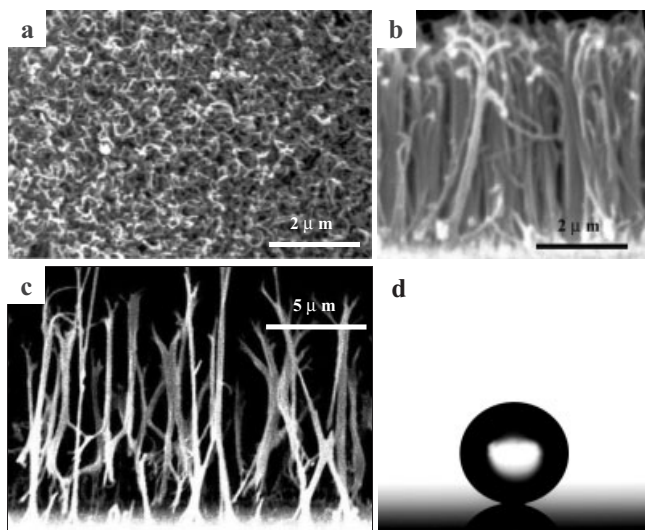


Fig. 2. a,b) SEM images of densely packed ACNT films (top view (a) and cross-sectional view (b)). Reproduced from [20] with permission from Wiley-VCH. c) SEM image of the cross section of PAN nanofibers. d) Shape of water droplet on the surface of as-synthesized PAN nanofibers. Reproduced from [21] with permission from Wiley-VCH.

These PAN nanofibers had a nanostructure similar to that of the ACNTs but a much lower density. This structure contributed to the very large fraction of air in the surface, which is essential to super-hydrophobicity.^[22] As a result, the value of CA on the surface of PAN nanofibers was as high as $173.8^\circ \pm 1.3^\circ$, even without any modification of this surface by materials of low surface energy (Fig. 2d). The needle-like structure proved to be an ideal surface for super-hydrophobicity.

The study of ACNT films and PAN nanofibers revealed that nanostructures on the surface are effective for obtaining large CAs. These results can be explained by Equation 1, i.e., without the terms f_s and f_v , the surface roughness can be enhanced by the nanostructures themselves, thus yielding a large CA. However, the value of α , the difference between advancing and receding CAs, was higher than 30° for water on both untreated ACNT films and a surface of PAN nanofibers. The reason is that water droplets are normally pinned on these nanostructured surfaces. More importantly, we are about to report for the first time the creation of a super-hydrophobic nanostructured surface from an amphiphilic polymer.^[23] This phenomenon is attributed to the rearrangement of poly(vinyl alcohol) (PVA) molecules during the extruding process, as well as the reorientation of hydrophobic groups ($-\text{CH}_2-$) at the air–solid interface. The study might open up new perspectives in the preparation of super-hydrophobic surfaces from various types of materials.

4. Low Sliding Angle Caused by Nano- and Microstructures

The hierarchical structures created by nanostructures on microstructures give a novel approach to constructing super-hydrophobic surfaces as in the natural world. Accordingly, lo-

tus-like ACNT films with both large CA and small α have been prepared. Figure 3a shows the SEM image of the top view of the lotus-like ACNT films; the average diameter of

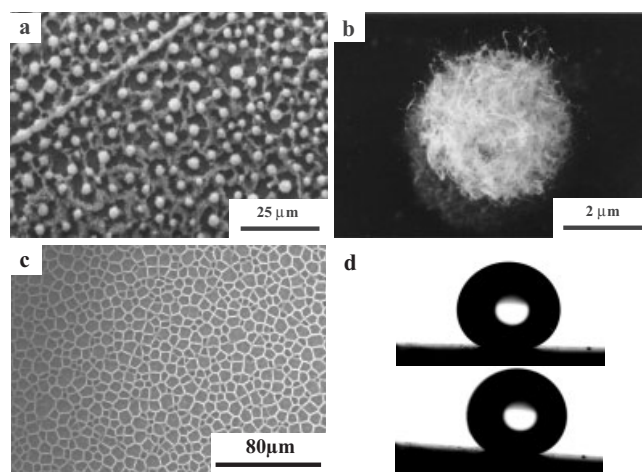


Fig. 3. a) SEM image of the top view of the lotus-like ACNT films. b) Enlarged view of a single papilla from (a). c) SEM image of the large-area honeycomb-like ACNT films. Reproduced from [24a] with permission from the American Chemical Society. d) Sliding behavior of a water droplet on the as-prepared lotus-like ACNT films (drop weight, 9 mg; tilt angle of surface, 3° ; high-speed photograph with 20 ms per frame).

the papillae and their separation were about $2.89 \pm 0.32 \mu\text{m}$ and $9.61 \pm 2.92 \mu\text{m}$, respectively. The HRSEM image of one single micropapilla with nanostructures is shown in Figure 3b. The outer diameter of the carbon nanotube was in the range from 30 to 60 nm (estimated from transmission electron microscopy (TEM) images of single carbon nanotubes, not shown here). CA on these ACNT films was about 166° , and α was about 3° . The lotus-like ACNT films have both a larger CA and a lower α , namely, anti-adhesion to water. These two aspects are both important for a super-hydrophobic surface. In comparison, the value of α on the lotus-like ACNT films was much lower than that on densely packed ACNT films with only nanostructures. The reason is that discrete contact was built up between the solid and liquid surfaces, which impacts the contour, length, and continuity of the triple contact line (TCL) around water droplets, consequently leading to the drastic decrease of α .^[6,7]

Based on this study, other patterned surfaces, including honeycomb-like, island-like, and post-like ACNT films with micro- and nanostructures, were prepared.^[24] Figure 3c shows a typical SEM image of as-synthesized large-area honeycomb-like ACNTs, whose surface exhibited super-hydrophobicity with high CA $163.4^\circ \pm 1.4^\circ$ and low α (less than 5°). The diameter of the honeycombs ranged from 3 to 15 μm . TEM investigation suggested that these honeycombs consisted of multi-walled nanotubes with a hollow inside; the diameter of a single carbon tube was about 25–50 nm. Figure 3d shows the sliding behavior of a water droplet on the as-prepared lotus-like ACNT films. Water droplets were unstable with respect to remaining on the surface, and spontaneously rolled off with a slight tremble.

5. The Effect of the Arrangement of Microstructures on Anisotropic Dewetting

Anisotropic wetting and dewetting are very important properties on patterned surfaces that have recently attracted much interest.^[25] In plants, it is well known that a water droplet can roll freely in all directions on the surface of a lotus leaf. However, we recently found an anisotropic dewetting tendency on the surface of a rice leaf.^[26] It is considered that the arrangement of micropapillae on this surface could influence the motions of water droplets. Figure 4a shows a large-scale SEM image of the surface of a rice leaf (the inset

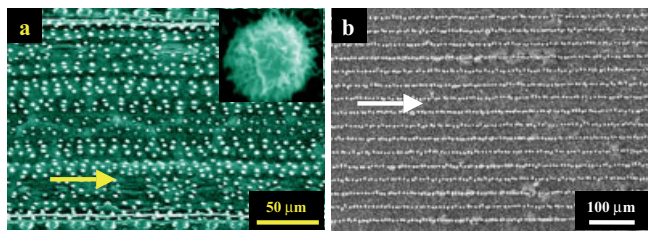


Fig. 4. a) Large-scale SEM images of the surface of a rice leaf (*Oryza sativa*) with different magnifications. b) SEM image of the top view of a rice-like ACNT film.

is a HRSEM image of an individual papilla), which has micro- and nanostructures similar to those of the lotus leaf. The papilla are arranged in one-dimensional order parallel to the leaf edge (direction of arrow) and randomly in the other directions (perpendicular to the arrow). The value of α was different for water rolling along the direction of the arrow (3° – 5°) and perpendicular to the arrow (9° – 15°). The TCL of the location of water droplets should be the main factor influencing α . On the surface of a rice leaf, TCL is influenced by the micropapillae arrangement. In comparison, TCL is similar in all directions for the homogeneous and random distribution of micropapillae on the surface of a lotus leaf. These results offered important information for designing for controllable wettability on a solid surface. Accordingly, we prepared the rice-like ACNT films shown in Figure 4b. The ordered pattern of these films was in two dimensions with different spacings. The water droplets rolled readily across the larger spacings (along arrow direction). Other types of pattern can also be obtained as desired. A lateral micro- and nanostructure surface can be fabricated by local growth of packed ACNTs. In this way, we can prepare a useful patterned surface by tuning the parameters, which makes the building of super-hydrophobic nanochannels possible.

6. Conclusion

This paper gives a brief review of recent progress in super-hydrophobic surfaces. Studies of the surface of plant leaves provide a novel approach to constructing super-hydrophobic

surfaces as in the natural world. Nanostructures are essential in fabricating super-hydrophobic surfaces with high CA, and multiscale structures can effectively reduce α of water droplets. Moreover, the arrangement of micro-array structures can influence how water droplets tend to move on these surfaces. Further efforts should concentrate on the application of super-hydrophobic surfaces to textiles,^[27] coatings,^[28] gene delivery,^[29] microfluidic channels,^[30] and non-wetting liquid transfer.^[31]

- [1] L. Jiang, R. Wang, B. Yang, T. J. Li, D. A. Tryk, A. Fujishima, K. Hashimoto, D. B. Zhu, *Pure Appl. Chem.* **2000**, *72*, 73.
- [2] R. Wang, K. Hashimoto, A. Fujishima, M. Chikuni, E. Kojima, A. Kitamura, M. Shimohigoshi, T. Watanabe, *Nature* **1997**, *388*, 434.
- [3] A. Fujishima, K. Hashimoto, T. Watanabe, *TiO₂ Photocatalyst, Fundamentals and Applications*, BKC, Tokyo **1999**.
- [4] A. Nakajima, K. Hashimoto, T. Watanabe, *Monatsh. Chem.* **2001**, *132*, 31.
- [5] A. Nakajima, A. Fujishima, K. Hashimoto, T. Watanabe, *Adv. Mater.* **1999**, *11*, 1365.
- [6] T. Onda, S. Shibuchi, N. Satoh, K. Tsujii, *Langmuir* **1996**, *12*, 2125.
- [7] W. Chen, A. Y. Fadeev, M. C. Heieh, D. Öner, J. Youngblood, T. J. McCarthy, *Langmuir* **1999**, *15*, 3395.
- [8] Y. Wu, H. Sugimura, Y. Inoue, O. Takai *Chem. Vap. Deposition* **2002**, *8*, 47.
- [9] K. Tsujii, T. Yamamoto, T. Onda, S. Shibuchi, *Angew. Chem. Int. Ed. Engl.* **1997**, *36*, 1011.
- [10] K. Tadanaga, N. Katata, T. Minami, *J. Am. Ceram. Soc.* **1997**, *80*, 3213.
- [11] A. Nakajima, K. Abe, K. Hashimoto, T. Watanabe, *Thin Solid Films* **2000**, *376*, 140.
- [12] J. Bico, C. Marzolin, D. Quéré, *Europhys. Lett.* **1999**, *47*, 220.
- [13] M. Miwa, A. Nakajima, A. Fujishima, K. Hashimoto, T. Watanabe, *Langmuir* **2000**, *16*, 5754.
- [14] a) W. Barthlott, C. Neinhuis, *Planta* **1997**, *202*, 1. b) C. Neinhuis, W. Barthlott, *Ann. Bot.* **1997**, *79*, 667.
- [15] P. Ball, *Nature* **1999**, *400*, 507.
- [16] J. Zhai, H. J. Li, Y. S. Li, S. H. Li, L. Jiang, *Physics* **2002**, *31*, 483.
- [17] A. W. Adamson, A. P. Gast, *Physical Chemistry of Surfaces*, Wiley, New York **1997**.
- [18] B. B. Mandelbrot, *The Fractal Geometry of Nature*, Freeman, San Francisco, CA **1982**.
- [19] W. Barthlott, C. Neinhuis, D. Cutler, F. Ditsch, I. Meusel, I. Theisen, H. Wilhelm, *Bot. J. Linn. Soc.* **1998**, *126*, 237.
- [20] a) H. Li, X. Wang, Y. Song, Y. Liu, Q. Li, L. Jiang, D. Zhu, *Angew. Chem. Int. Ed.* **2001**, *40*, 1743; *Angew. Chem.* **2001**, *113*, 1793. b) H. Li, X. Wang, Y. Song, Y. Liu, Q. Li, L. Jiang, D. Zhu, *Chem. J. Chin. Univ.* **2001**, *22*, 759.
- [21] L. Feng, S. Li, H. Li, J. Zhai, Y. Song, L. Jiang, D. Zhu, *Angew. Chem. Int. Ed.* **2002**, *41*, 1221; *Angew. Chem.* **2002**, *114*, 1269.
- [22] A. B. D. Cassie, *Discuss. Faraday Soc.* **1948**, *44*, 11.
- [23] L. Feng, Y. Song, J. Zhai, B. Liu, J. Xu, L. Jiang, D. Zhu, *Angew. Chem.*, in press.
- [24] a) S. Li, H. Li, X. Wang, Y. Song, Y. Liu, L. Jiang, D. Zhu, *J. Phys. Chem. B* **2002**, *106*, 9274. b) S. Li, L. Feng, H. Li, Y. Song, L. Jiang, D. Zhu, *Chem. J. Chin. Univ.*, in press. c) S. Li, H. Liu, H. Li, J. Zhai, Y. Song, L. Jiang, D. Zhu, *Chem. J. Chin. Univ.*, in press.
- [25] a) M. Gleiche, L. F. Chi, H. Fuchs, *Nature* **2000**, *403*, 173. b) A. M. Higgins, R. A. L. Jones, *Nature* **2000**, *404*, 476.
- [26] Y. Li, L. Feng, S. Li, L. Zhang, L. Jiang, D. B. Zhu, unpublished.
- [27] D. Cyranoski, *Nature* **2001**, *414*, 240.
- [28] A. Duparré, M. Flemming, J. Steinert, K. Reih, *Appl. Opt.* **2002**, *41*, 3294.
- [29] C. M. Henry, *Chem. Eng. News* **2001**, *79*, 35.
- [30] H. Kind, J. M. Bonard, C. Emmenegger, L. O. Nilsson, K. Hermadi, S. E. Maillard, L. Schlapbach, L. Forro, K. Kern, *Adv. Mater.* **1999**, *11*, 1285.
- [31] H. Gau, S. Herminghaus, P. Lenz, R. Lipowsky, *Science* **1999**, *283*, 46.